Cavitating Pump Performance

A typical non-cavitating performance characteristic for a centrifugal pump is shown in figure 1 for the
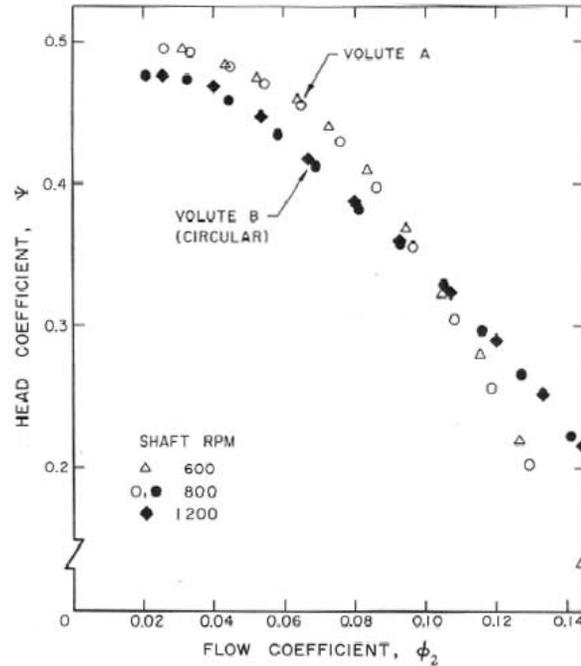
Figure 1: Typical non-cavitating performance for a centrifugal pump, namely Impeller X (see section (Mbbi)) with Volute A and a circular volute of uniform cross-section (from Chamieh 1983).

Impeller X/Volute A combination (Chamieh 1983) described in section (Mbbi). The design flow coefficient for this pump is $\phi_2 = 0.092$ but we note that it performs reasonably well down to about 30% of this design flow. This flexibility is characteristic of centrifugal pumps. Data is presented for three different shaft speeds, namely 600, 800 and 1200rpm; since these agree closely we can conclude that there is no perceptible effect of Reynolds number for this range of speeds. The effect of a different volute is also illustrated by the data for Volute B which is a circular volute of circumferentially uniform area. In theory this circular volute is not well matched to the impeller discharge flow and the result is that, over most of the range of flow coefficient, the hydraulic performance is inferior to that with Volute A. However, Volute B is superior at high flow coefficients. This suggests that the flow in Volute A may be more pathological than one would like at these high flow coefficients (see sections (Mbdd) and (Mbde)). It further serves to emphasize the importance of a volute (or diffuser) and the need for an understanding of the flow in a volute at both design and off-design conditions.

Typical cavitation performance characteristics for a centrifugal pump are presented in figure 2 for the Impeller X/Volute A combination. The breakdown cavitation numbers in the range $\sigma = 0.1 \rightarrow 0.4$ are consistent with the data in table 1, section (Mbee). Note that the cavitation head loss occurs more gradually at high flow coefficients than at low values. This is a common feature of the cavitation performance of many pumps, both centrifugal and axial.

Now consider some examples of axial and mixed flow pumps. Typical non-cavitating performance characteristics are shown in figure 3 for a Peerless axial flow pump. This unshrouded pump has a design flow coefficient $\phi_2 = 0.171$. The maximum efficiency at this design point is about 85%. Axial flow pumps
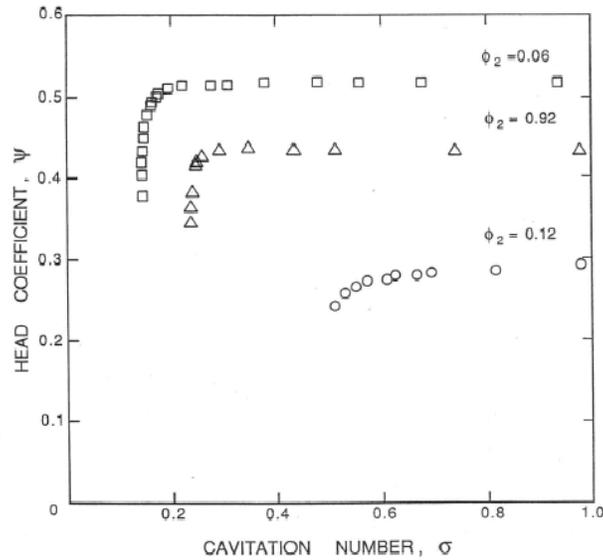
Figure 2: Cavitation performance for the Impeller X/Volute A combination (from Franz *et al.* 1989, 1990). The flow separation rings of figure **??** have been installed so the non-cavitating performance is slightly better than in figure 1.
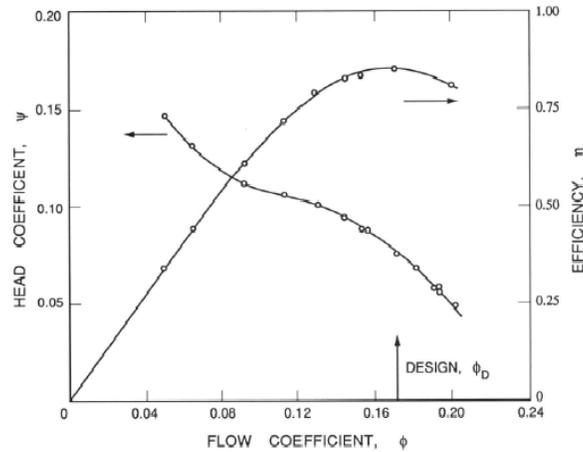
Figure 3: Typical non-cavitating performance characteristics for a $20.3cm$ diameter, 3-bladed axial flow pump with a hub-tip ratio, R_H/R_T, of 0.45 running at about $1500rpm$. At the blade tip the chord is $7.3cm$, the solidity is 0.344 and the blade angle, β_{bT}, is 11.9°. Adapted from Guinard *et al.* (1953).

are more susceptible to flow separation and stall than centrifugal pumps and could therefore be considered less versatile. The depression in the head curve of figure 3 in the range $\phi_2 = 0.08 \rightarrow 0.12$ is indicative of flow separation and this region of the head/flow curve can therefore be quite sensitive to the details of the blade profile since small surface irregularities can often have a substantial effect on separation. This is illustrated by the data of figure 4 which presents the non-cavitating characteristics for four similar axial flow pumps with slightly different blade profiles. The kinks in the curves are more marked in this case and differ significantly from one profile to another. Note also that there are small regions of positive slope in the head characteristics. This often leads to instability and to fluctuating pressures and flow rates through the excitation of the surge and stall mechanisms discussed in the following chapters. Sometimes the region of positive slope in the head characteristic can be even more marked as in the example presented in figure 5 in which the stall occurs at about 80% of the design flow. As a final example of non-cavitating performance we include in figure 6, the effect of the blade angle in an axial flow pump; note that angles of the order of 20° to 30° seem to be optimal for many purposes.
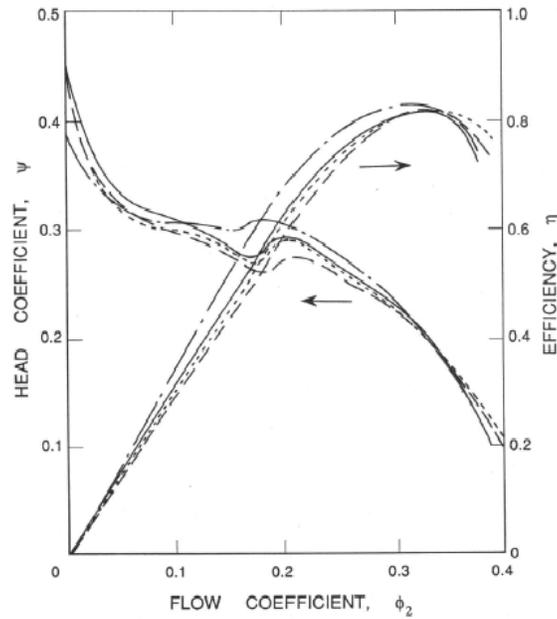
Figure 4: Typical non-cavitating performance characteristics for a four-bladed axial flow pump with tip blade angle, β_{bT}, of about 18°, a hub-tip ratio, R_H/R_T, of 0.483, a solidity of 0.68 and four different blade profiles (yielding the set of four performance curves). Adapted from Oshima and Kawaguchi (1963).
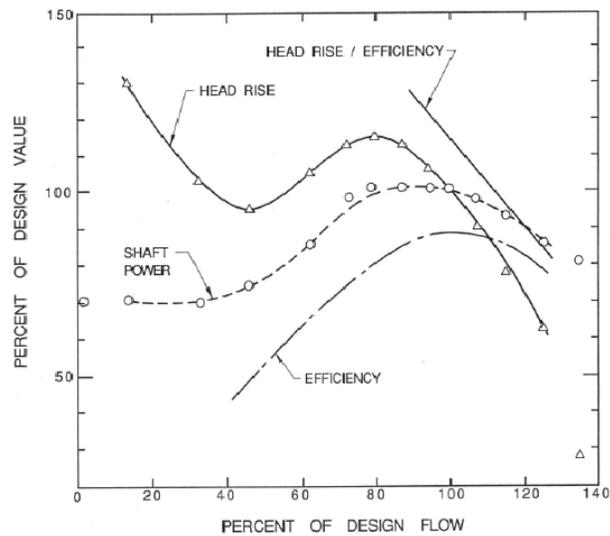
Figure 5: Characteristics of a mixed flow pump (Myles 1966).

The cavitation characteristics for some of the above axial flow pumps are presented in figures 7 through 10. The data of Guinard *et al.* (1953) provides a particularly well-documented example of the effect of cavitation on an axial flow pump. Note first from figure 7 that the cavitation inception number is smallest at the design flow and increases as ϕ is decreased; the decrease at very low ϕ does not, however, have an obvious explanation. Since Guinard *et al.* (1953) noticed the hysteretic effect described in section (Mbec) we present figure 8 as an example of that phenomenon.

The cavitation data of figure 7 also help to illustrate several other characteristic phenomena. Note the significant increase in the head just prior to the decrease associated with breakdown. In the case of the pump tested by Guinard *et al.*, this effect occurs at low flow coefficients. However, other pumps exhibit this phenomenon at higher flows and not at low flows as illustrated by the data of Oshima and Kawaguchi
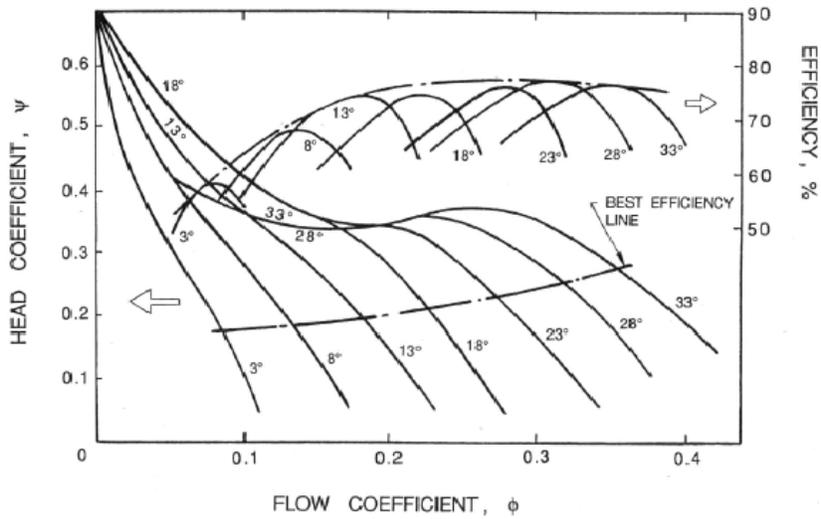
Figure 6: Head and efficiency characteristics for an axial flow pump with different tip blade angles, β_{bT} (from Peck 1966).
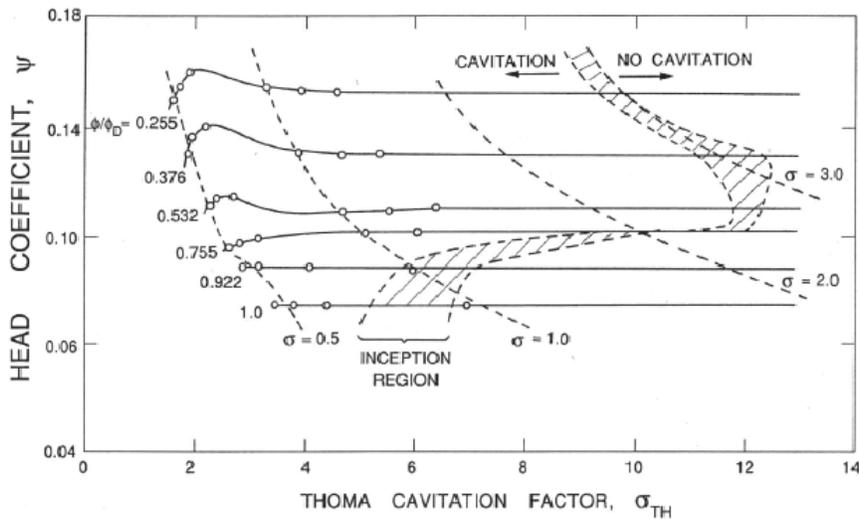
Figure 7: Cavitation performance characteristics of the axial flow pump of figure 3. Adapted from Guinard *et al.* (1953).

(1963) presented in figure 9. The effect is probably caused by an improved flow geometry due to a modest amount of cavitation.

The cavitation data of figure 7 also illustrates the fact that breakdown at low flow coefficients occurs at higher cavitation numbers and is usually more abrupt than at higher flow coefficients. It is accompanied by a decrease in efficiency as illustrated by figure 9. Finally we include figure 10 which shows that the effect of blade profile changes on the head breakdown cavitation number is quite small.
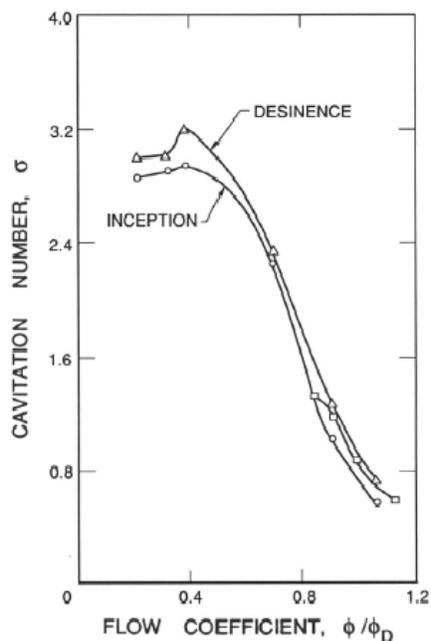
Figure 8: Inception and desinent cavitation numbers (based on w_{T1}) as a function of ϕ/ϕ_D for the axial flow pump of figures 3 and 7. Adapted from Guinard *et al.* (1953).
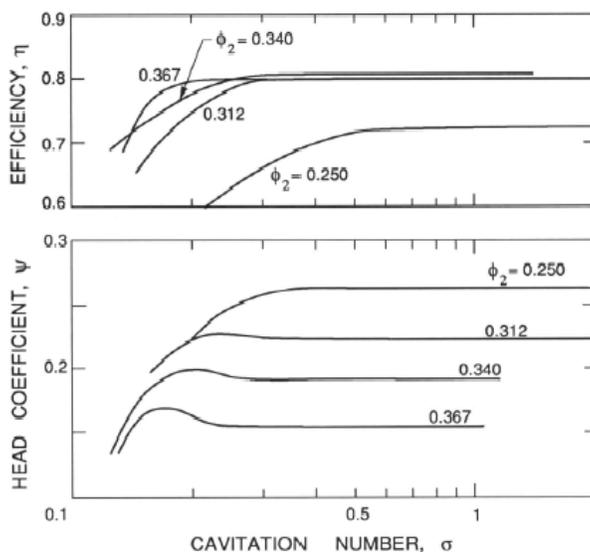
Figure 9: Effect of cavitation on the head coefficient and efficiency of one of the axial flow pumps of figure 4. The cavitation number is based on w_{T1}. Adapted from Oshima and Kawaguchi (1963).
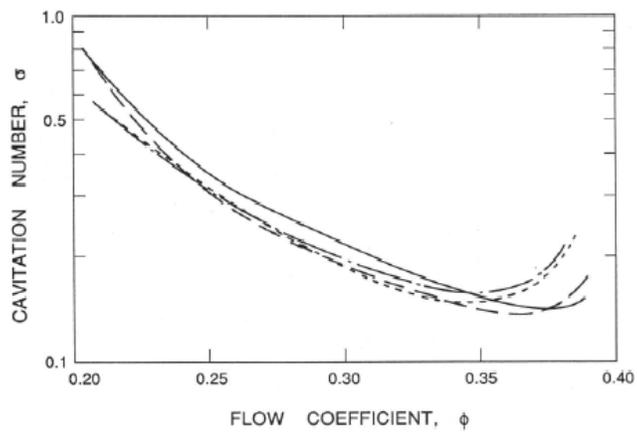
Figure 10: The critical cavitation number (based on w_{T1} and 0.5% head loss) for the axial flow pumps of figure 4. Adapted from Oshima and Kawaguchi (1963).